ELSEVIER

PII: S0144-8617(96)00042-2

Carbohydrate Polymers **30** (1996) 55–60

0144-8617/96/$15.00 + .00

Investigation, using analytical ultracentrifugation, of the effect of the incorporation of the fluorophore 9-anthraldehyde on two chitosans of differing degrees of acetylation

Helmut Cölfen,[a,c] Stephen E. Harding[a]* & Kjell-M. Vårum[b]

[a]*National Centre for Macromolecular Hydrodynamics, University of Nottingham, Department of Applied Biochemistry and Food Science, Sutton Bonington, LE12 5RD, UK*
[b]*Universitetet i Trondheim, Institutt for bioteknologi, N-7034 Trondheim, Norway*
[c]*Present address: Max-Planck Institute for Colloid and Interface Research, Colloid Chemistry Department, Kanstr. 55, D-14513 Teltow, Germany*

(Received 17 June 1995; revised version received 1 September 1995; accepted 27 September 1995)

1. Incorporation of the fluorophore 9-anthraldehyde onto chitosans has been considered as potentially advantageous in terms of visualisation both in biomedical applications and molecular characterisation. 2. the effect of increase in degree of substitution of the fluorophore has been investigated on 2 chitosans of differing degrees of acetylation by analytical ultracentrifugation. 3. homogeneity and sedimentation coefficient evaluations by sedimentation velocity and apparent molar mass measurements by sedimentation equilibrium suggest no change in molar mass, but a slight change in conformation to a more compact state. 4. accidentally produced 'Toepler–Schlieren images' have been generated using a new commercially available analytical ultracentrifuge equipped with only scanning absorption optics. Copyright © 1996 Elsevier Science Ltd

INTRODUCTION

One of the problems encountered when attempting to visualise the presence of polysaccharides — either for characterisation purposes (such as by analytical ultracentrifugation) or for detection purposes in their various applications — is that they are usually transparent to the visible and (useable) ultraviolet parts of the electromagnetic spectrum. One possible way of overcoming this invisibility is to label the polysaccharide with a chromophore; a labelling procedure which has been widely used in the protein biochemistry field and recently extended to polysaccharides. For example, dextrans are widely used as blood plasma subsitutes and been considered for site-specific drug-delivery (Harboe *et al.*, 1989); to visualise their distribution in the body a γ-ray emitting label (di-iodotyrosine) has been incorporated. Using the UV absorption of the tyrosine part, Errington *et al.* (1992) showed that the incorporation of the di-iodotyrosine label had definite effects on the hydrodynamic properties of the dextran. A similar rationale is behind the present study. Chitosans are increasingly being considered in biomedical and pharmaceutical applications (see, e.g. Fiebrig *et al.*, 1994; Artursson *et al.*, 1994) and to help visualise them *in vivo*, Kenne *et al.* (1995) have labelled chitosans at different degrees of acetylation with the fluorophore 9-anthraldehyde (Fig. 1). This fluorophore has an absorption maxima at a wavelength of ~250nm. The aim of this present study is to investigate the effect on hydrodynamic properties on two of these chitosans at

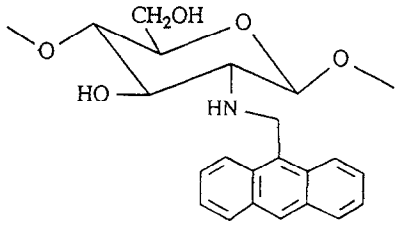

Fig. 1. 9-anthraldehyde chitosan. 9-anthraldehyde was coupled to the chitosans by the process of reductive amination to an NH_2 residue.

*Corresponding author: Tel, 00 44 1159 516148; fax, 00 44 1159 516142; e-mail, sczsteve@sznl.nott.ac.uk

widely different degrees of acetylation ['Chitosan 1' of degree of acetylation, $F_A = 0.15$ (15%) and 'Chitosan 2', $F_A = 0.61$] in terms of the sedimentation coefficient and apparent weight average molar mass. The incorporation of the chromophore is particularly advantageous in that it allows the use of a new commercially available analytical ultracentrifuge which is equipped, at the present time, with only scanning absorption optics.

MATERIALS AND METHODS

9-anthraldehyde chitosan

Chitosans of differing degrees of acetylation (F_A), 'Chitosan 1' [$F_A = 0.15$ (15%)] and [Chitosan 2] [$F_A = 0.61$ (61%)] were labelled with the hydrophobic chromophore 9-anthraldehyde by the technique of reductive amination (Kenne et al., 1995). This was done for each chitosan to three degrees of substitution: ~0.01, ~0.1 and ~1%, with the amount of label incorporated assayed by its absorption at a wavelength of 253.7nm, where the labelled chitosan has a strong absorption maximum.

Solutions

An acetate buffer was initially made up with the following composition (Dawson *et al.*, 1986): 0.04 M CH_3COONa, 0.04 M CH_3COOH and 0.2 M NaCl. The chitosans were solubilised in deionised distilled water at double the desired stock concentration, and then an equal volume of buffer added to yield a final buffer pH of 4.1 and ionic strength slightly above 0.1

Analytical ultracentrifugation

Three analytical ultracentrifuges were used: The new Beckman Optima XL-A ultracentrifuge equipped with scanning absorption optics (Giebler, 1992) and two conventional Beckman Model E ultracentrifuges, one dedicated to classical phase-plate or 'Philpot–Svensson' optics, the other, equipped with a 5 mW He–Ne laser, dedicated to Rayleigh interference optics (see, e.g. Lloyd, 1974)

Sedimentation velocity

Sedimentation velocity experiments (homogeneity tests and sedimentation coefficient evaluations) were performed on the Optima XL-A ultracentrifuge and the particular Model E dedicated to phase-plate Schlieren optics. For experiments using the absorption optical system of the Optima XL-A a rotor speed of 50 000 rev/min, running temperature of 20.0°C and scanning wavelengths of 250 nm and 370 nm were employed. The scans were analysed using a QUICKBASIC algorithm SEDVEL which gives the apparent sedimentation coefficient $s_{20,b}$ at a concentration c (mg/ml) and the radial dilution factor (Schachman, 1959 pp. 70–73). $s_{20,b}$ values, where the subscript 'b' means 'in the buffer' were corrected to standard conditions (to the case if the buffer had the same density and viscosity of water at 20°C) using the well-known formula (see e.g. Tanford, 1961):

$$s_{(20,w)} = \frac{(1 - \bar{\nu}\rho)_{20,w}}{(1 - \bar{\nu}\rho)_{T,b}} \cdot \frac{\eta_{T,b}}{\eta_{20,w}} \cdot s_{T,b}, \quad (1)$$

where ρ is the solvent density, η the solvent viscosity and $\bar{\nu}$ is the partial specific volume of the chitosan, taken to be 0.565 ml/g (Errington *et al.*, 1993).

For measurements on the Model E rotor speeds of 48,000 rev/min and 56,000 rev/min were chosen, again at a temperature of 20°C. The following method of semi-automatic data capture was employed. Photographs were taken at 32 min intervals in each case, and negatives enlarged directly onto a graphics tablet interfaced to an IBM-PC. The resulting records of the position of the sedimenting boundaries could then be analysed using the QUICKBASIC algorithm MOD_EVEL (Cölfen unpublished) to yield the (apparent) sedimentation coefficients $s_{20,b}$, which were then corrected to $s_{20,w}$ values according to eqn (1) above. As has been reported earlier (Cölfen & Harding, 1995) it is possible to obtain in some cases Toepler-type Schlieren images from the XL-A ultracentrifuge using the absorption optical system (without a proper knife-edge or phase-plate) under certain conditions and wavelengths away from absorption maxima: in this study advantage was taken of this feature to provide a further check on the $s_{20,w}$ values.

Because relative (i.e. as a function of the degree of substitution) rather than absolute effects were the object of this study (and also because of scarcity of material), $s_{20,w}$ values were measured at one single concentration of chitosan (2 mg/ml) and concentration dependencies were not investigated.

In both cases (XL-A and Model E) samples were run in multiples of 3 using four-hole rotors (one hole used for the counterbalance/reference cell) and either the multiplexing system for the XL-A or the use of cells with wedge windows for the Beckman Model E.

Sedimentation equilibrium

Used for determination of the apparent (i.e. at finite concentration) weight average molar masses. As above, both absorption and refractometric optics were used, although with the latter, the Rayleigh interference optical system rather than Schlieren was used because of its greater precision and sensitivity for sedimentation equilibrium work. Apparent weight average molar masses were determined at a temperature of 20°C and concentration of 2 mg/ml in 10 mm optical path length double

sector cells, with dialysate in the reference sectors. As with other measurements on polysaccharides, because of the inherent polydispersity of the chitosans, the high speed or meniscus depletion method was avoided to ensure proper optical registration at the cell base (Creeth & Harding, 1982). Instead, the 'intermediate speed' method was used (Creeth & Harding, 1982), where the concentration at the meniscus remains finite and the absorption (absorption optics) or fringe displacement (Rayleigh optics) at the cell base is retained within the limits of optical registration.

Sedimentation equilibrium experiements were used for determination of apparent molar masses using the absorption optical system of the Optima XL-A; rotor speeds of 18,000 and 20,000 rev/min were used at scanning wavelength of 250 nm. The absorption data were interpreted using the routine MSTARA (Harding *et al.*, 1992) now available in QUICKBASIC (Cölfen & Harding, 1995). This, amongst other things, yields the apparent weight average molar mass, $M_{w,app}$ from use of the operational point average known as M^* (Creeth & Harding, 1982).

For the determination of the apparent molar masses using the Rayleigh interference optical system of the Beckman Model E a rotor speed of 18,000 rev/min was employed. Solute distributions at sedimentation equilibrium were recorded photographically and then captured onto a PC by an Ultroscan (LKB, Bromma, Sweden) enhanced laser scanning densitometer. Fringe profiles were then converted into an accurate record of fringe displacement against radial displacement using a TURBO-PASCAL Fourier cosine series algorithm known as ANALYSER (Harding & Rowe, 1988; Rowe *et al.*, 1992) and then interpreted using the routine MSTARI (Harding *et al.*, 1992; Cölfen & Harding, 1995) which is the version of MSTARA (see above) written for the Rayleigh Optical System.

RESULTS AND DISCUSSION

Homogeneity

From the sedimentation velocity scans at 250 nm single sedimenting boundaries were observed for both chitosans at all three degrees of substitution, suggesting that any polydispersity present was of the quasi-continuous as opposed to the discrete type. For chitosan 1 and chitosan 2 at 250 nm, conventional 'sigmoidal' absorption boundaries were observed (Fig. 2a); for chitosan 2, Toepler–Schlieren images were visible for all 3 degrees of substitution (nominal 0.01, 0.1 and 1% 9-anthraldehyde) at wavelengths of 280 nm and 370 nm (i.e. away from the absorption maxima), but again showing no evidence of discrete types of polydispersity (Fig. 2b,c) and consistent with the photographic records of conventional Philpott–Svensson phase-plate Schlieren boundaries obtained

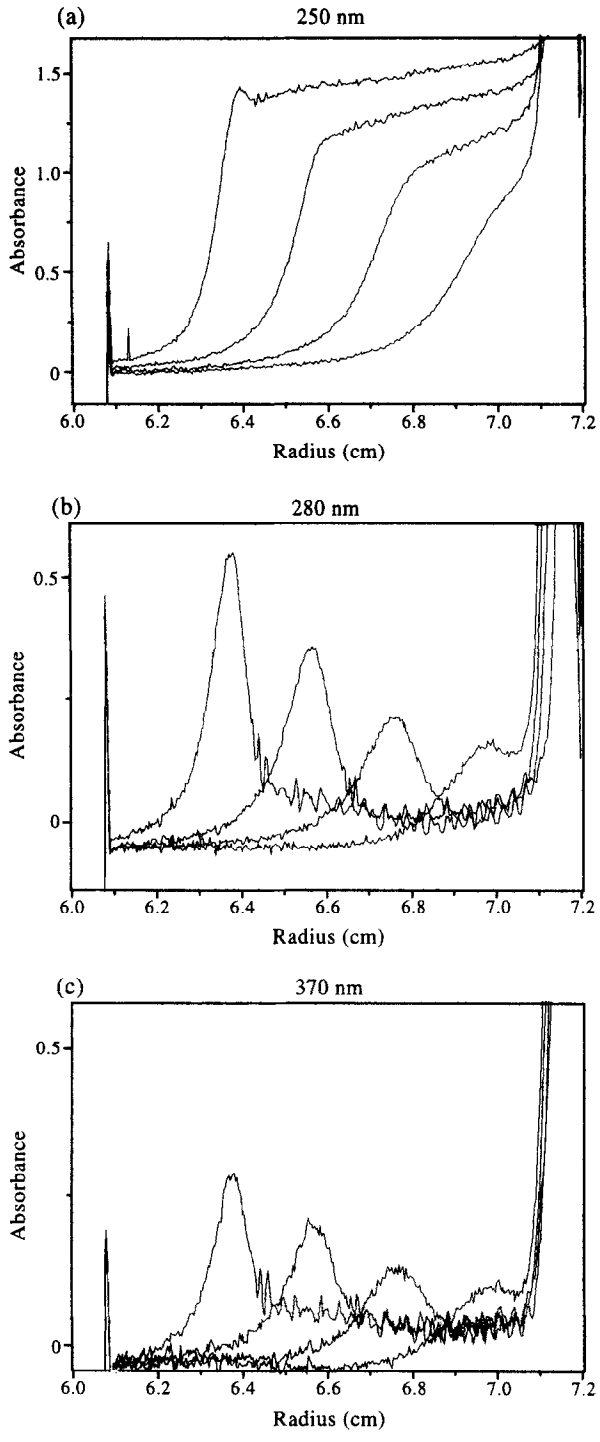

Fig. 2. Sedimentation velocity diagrams for Chitosan 2 ($F_A = 0.61$) from the absorption optical system of the XL-A ultracentrifuge. (a) wavelength = 250 nm (b) wavelength = 280 nm (c) wavelength = 370 nm. Degree of substitution = 1%. Rotor speed = 50,000 rev/min, temperature = 20°C, loading concentration = 2 mg/ml, scan interval = 120 min. Direction of sedimentation is from left to right.

from the Beckman Model E (Fig. 3). The height of the Toepler–Schlieren peaks was clearly wavelength dependent, whereas the position was not. Similar observations have been made on other polysaccharides (and bovine serum albumin) including an unlabelled chitosan (Cölfen

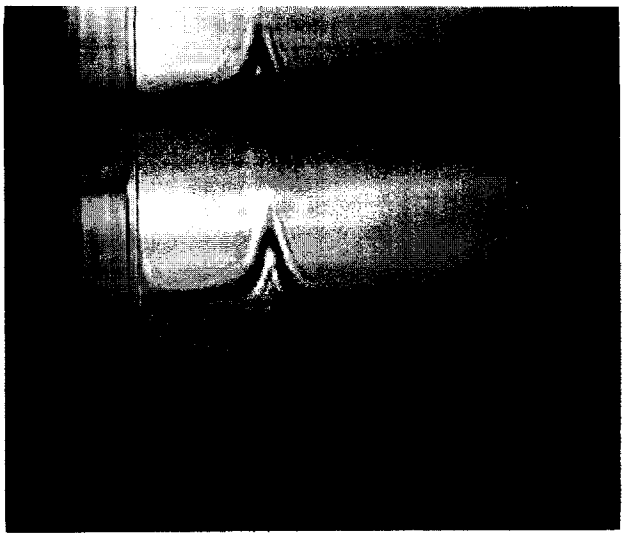

Fig. 3. Conventional phase-plate Schlieren images of chitosan 2 at a rotor speed of 48,000 rev/min from the Model E ultracentrifuge. Temperature = 20°C, loading concentration = 2 mg/ml. The upper sedimentation diagram corresponds to a degree of substitution, DS = 0.01%, the centre to DS = 0.1%, the lower to DS = 1%. Phase plate angle = 75°. Direction of sedimentation is from left to right.

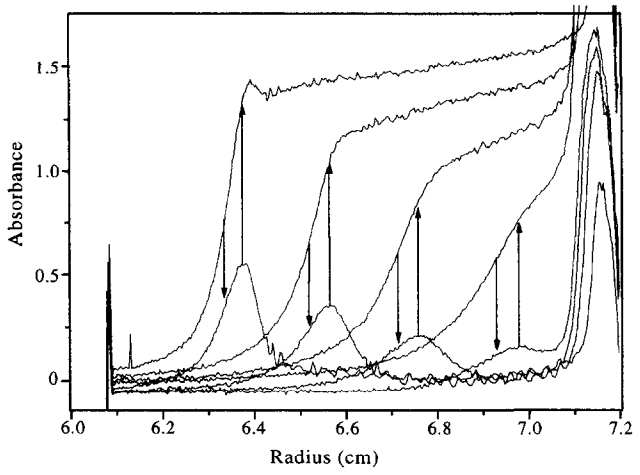

Fig. 4. Absorption and Toepler–Schlieren patterns derived with the XL-A absorption optics for chitosan 2, DS = 1% at wavelengths of 250 nm (normal absorption traces) and 280 nm (Toepler–Schlieren). The time delay between the scanning at the two wavelengths is negligible compared with the slow sedimentation. Time interval between scans = 120 min. Loading concentration = 2 mg/ml, rotor speed = 50,000 rev/min.

& Harding, 1995). Although the nature and generation of these type of Toepler–Schlieren images in the XL-A ultracentrifuge by macromolecules in general is the subject of a separate study (Cölfen & Harding, 1995) it is worth commenting here that even though the sedimenting Schlieren boundaries do appear slightly in advance of the conventional absorption boundary (Fig. 4) — a feature of their 'accidental' as opposed to 'designed' production — they do give very similar sedimentation coefficients. For example the "Schlieren images" of Fig. 4 give an $s_{20,w}$ of 1.77 S and the conventional absorption traces a value of 1.70 S. This adds to the view described earlier (Cölfen & Harding, 1995) that the (so far) 'accidental' production of Schlieren images by the optical system of the XL-A ultracentrifuge could form the basis of a commercially designed Schlieren system for this ultracentrifuge.

Table 1. Sedimentation coefficients as a function of degree of substitution (DS) for chitosan 1 (F_A = 0.15). Loading concentration = 2 mg/ml

	$s_{20,w}$ (Svedbergs) XL-A data (±~2%)	$s_{20,w}$ (Svedbergs) Model E data (±~2%)
DS~0.01%	1.41	1.43
DS~0.1%	1.49	1.49
DS~1%	1.39	1.52

Table 2. Sedimentation coefficients as a function of degree of substitution (DS) for chitosan 2 (F_A = 0.61). Loading concentration = 2 mg/ml

	$s_{20,w}$ (Svedbergs) XL-A data (±~2%)	$s_{20,w}$ (Svedbergs) Model E data (±~2%)
DS~0.01%	1.64	1.60
DS~0.1%	1.61	1.62
DS~1%	1.74	1.69

Sedimentation coefficients, $s_{20,w}$

Tables 1 and 2 compare the sedimentation coefficients (at a loading concentration of 2 mg/ml) as a function of the degree of substituition of the chromophore for the two chitosans. As can be clearly seen, results from the XL-A are in excellent agreement with those from the 'conventional Schlieren' optics of the Beckman Model E. Although this is not clear from the XL-A results, the more precise Model E data (Tables 1 and 2) suggest a subtle increase in the sedimentation coefficient with increase in degree of substitution for both chitosans: this would suggest an increase in the degree of compactness with increase in degree of substitution. This is consistent with the observed increase in the degree of boundary spreading (through increased diffusion) (Fig. 3). An explanation for these phenomena is that the incorporation of the highly hydrophobic fluorophore causes a change in conformation to shield the fluorophore from the hydrophilic environment of the solvent. An alternative explanation is a change in mass of the chitosans caused by self-association or some other effect, but this later hypothesis is refuted by the results from sedimentation equilibrium.

Sedimentation equilibrium: weight average molar masses, $M_{w,app}$

In order to obtain absolute molar mass information on the substituted chitosans conventional intermediate

Table 3. Apparent molar masses at 2 mg/ml from sedimentation equilibrium on the Model E ultracentrifuge (Rayleigh interference optics) as a function of degree of substitution (DS)

	$M_{w,app}$ (g/mol) Chitosan 1 (F_A = 0.15)	$M_{w,app}$ (g/mol) Chitosan 2 (F_A = 0.61)
DS = 0.01%	26,000±2000	39,000±5000
DS = 0.1%	24,500±500	40,000±5000
DS = 1%	23,000±1000	42,000±3000

speed sedimentation equilibrium results using the Rayleigh interferece optical system of the Beckman Model E showed clearly (Table 3) that increase of the degree of substitution of the fluorophore has no discernible effect on the apparent weight average molar mass, $M_{w,app}$ at a loading concentration of 2 mg/ml. Thus we can reasonably say that incorporation of the fluorophore has no deleterious effects on the mass of the two chitosans, making this derivative suitable for applications in biology (i.e. visualisation of chitosans in tissue by fluorescence microscopy). The less-precise absorption optical system on the XL-A on solutions at the same loading concentration (2 mg/ml) gave the same ball-park apparent molar masses, but in one case only to within ±50%, confirming that conventional Rayleigh interference optics should still be the method of choice for molar mass determinations. (The presence of unbound fluorophore in the solvent is probably not the explanation for this, since this is normally taken into account by overspeeding after the final equilibrium distribution has been recorded to obtain a baseline.) It should also be stressed that the molar masses quoted in Table 3 are *apparent* molar masses obtained at a rather high loading concentration, and, because of the well-known strong non-ideality of chitosan solutions (see, e.g. Errington *et al.*, 1993) are likely to be considerably lower than the "ideal values". This feature is borne out in the strong downward curvature of plots of the log of the fringe displacement versus concentration squared (Fig. 5) and would account for the apparent discrepancy with the relative molar masses determined from viscosity measurements (Anthonsen *et al.*, 1993) of ~250000 (Chitosan 1) and ~190000 (Chitosan 2) (Kenne *et al.*, 1995).

In summary: 1. the increased incorporation of the fluorophore 9-anthtraldehyde, at least up to a degree of substitution of 1% has no deleterious effect on the molar mass of two chitosans of differing degrees of acetylation. 2. There appears however to be a subtle change in conformation of both chitosans (on increasing the degree of substitution of the highly hydrophobic fluorophore) to a more compact state based on a small increase in sedimentation coefficient and increased boundary diffusion. 3. Incorporation of the fluorophore allows the use of the absorption optical system on an ultracentrifuge for evaluation of sedimentation velocity properties (homogeneity, sedimentation coefficient), although to a lower precision compared to conventional phase-plate Schlieren optics: this can miss subtle changes in conformation. Molar mass evaluations using the absorption optical system on these molecules are less reliable than the conventional Rayleigh interference procedure. 4. This study gives a further demonstration of the "accidental" production of Toepler–Schlieren images from the absorption optical system of the XL-A ultracentrifuge, an observation which should have commercial value for the design of a proper Schlieren system for this ultracentrifuge.

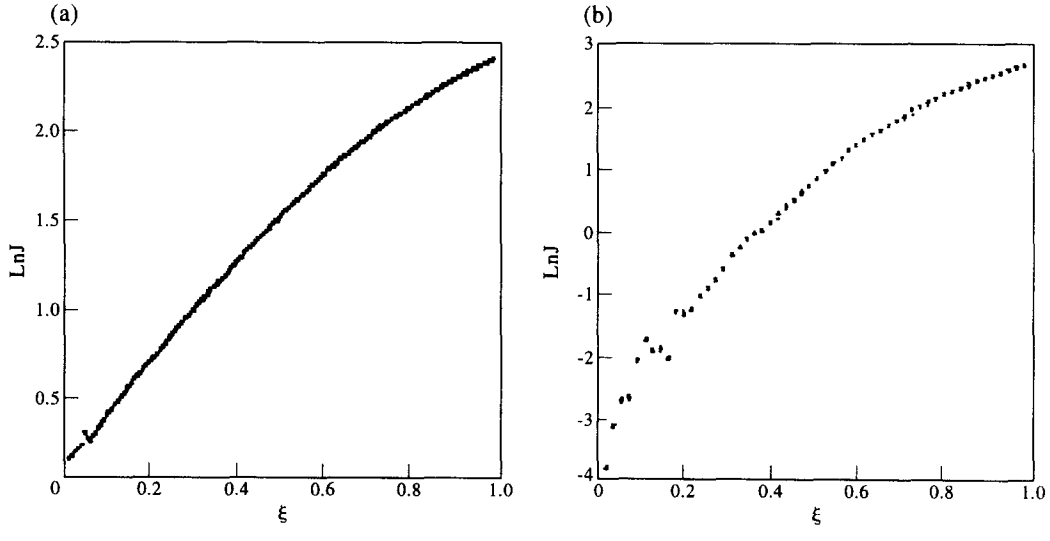

Fig. 5. Plot of the logarithm of the fringe displacement, J versus the normalised radial displacement squared parameter, ξ, at a loading concentration of 2.0 mg/ml. $\xi = (r^2 - a^2)/(b^2 - a^2)$ where r is the radial displacement from the centre of the rotor of a given point in the ultracentrifuge cell, and a and b the corresponding radial positions of the solution/air meniscus and the cell base respectively. (a) chitosan 1, DS = 0.01%, rotor speed = 18 000 rev/min. (b) chitosan 2, DS = 0.01%, rotor speed = 18 000 rev/min.

REFERENCES

Anthonsen, M.W., Vårum, K.M. & Smidsrød, O. (1993). Solution properties of chitosans: conformation and chain stiffness of chitosans with different degrees of N-acetylation. *Carbohyd. Polym.*, **22,** 193–201.

Artursson, P., Lindmark, T., Davis, S.S. & Illum, L. (1994). Effect of chitosan on the permeability of monolayers of intestinal epithelial cells (Caco-2). *Pharmaceutical Research,* **11,** 1358–1361.

Cölfen, H. & Harding, S.E. (1995). A study on Schlieren patterns derived with the Beckman Optima XL-A UV absorption optics. *Prog. Colloid Polym. Sci.*, **99,** 167–186.

Cölfen, H. & Harding, S. E. (1996). In press.

Creeth, J.M. & Harding, S.E. (1982). Some observations on a new type of point average molecular weight. *J. Biochem. Biophys. Meth.*, **7,** 25–34.

Dawson, R. M. C., Elliott, D. C., Elliott, W. H. & Jones, K. M. (1986). *Data for Biochemical Research* (3rd edition). Oxford University Press, p. 429.

Errington, N., Harding, S.E., Illum, L. & Schacht, E.H. (1992). Physico-chemical studies on di-iodotyrosine dextran. *Carbohyd. Polym.*, **18,** 289–294.

Errington, N., Harding, S.E., Vårum, K.-M. & Illum, L. (1993). Hydrodynamic characterisation of chitosans of differing degrees of acetylation. *Int. J. Biol. Macromol.*, **15,** 113–117.

Fiebrig, I., Harding, S.E. & Davis, S.S. (1994). Sedimentation analysis of potential interactions between mucins and a putative bioadhesive polymer. *Prog. Colloid Polym. Sci.*, **94,** 66–73.

Giebler, R. (1992) The Optima XL-A: A new analytical ultracentrifuge with a novel precision absorption optical system. In *Analytical Ultracentrifugation in Biochemistry and Polymer Science*, eds. S. E. Harding, A. J. Rowe & J. C. Horton. Chapter 2, Royal Society of Chemistry, Cambridge, UK.

Harboe, E., Larsen, C., Johansen, M. & Olesen, H. (1989). *Pharm. Res.*, **6,** 919–923.

Harding, S. E., Horton J. C. & Morgan, P. J. (1992). MSTAR: A FORTRAN program for the model independent molecular weight analysis of macromolecules using low speed or high speed sedimentation equilibrium. In *Analytical Ultracentrifugation in Biochemistry and Polymer Science*, eds. S. E. Harding, A. J. Rowe & J. C. Horton. Chapter 15, Royal Society of Chemistry, Cambridge, UK.

Harding, S.E. & Rowe, A.J. (1988). Automatic data capture and analysis of Rayleigh interference displacements in analytical ultracentrifugation. *Optics and Lasers in Engineering,* **8,** 83–96.

Harding, S.E., Vårum, K.-M., Stokke, B.T. & Smidsrød, O. (1991). Molecular weight determination of polysaccharides. *Advances in Carbohydrate Analysis,* **1,** 63.

Kenne, L., Tian, W. & Vårum, K. M. (1995). In preparation.

Lloyd, P. H. (1974). *Optical Methods in Ultracentrifugation, Electrophoresis and Diffusion* Oxford University Press.

Rowe, A. J. Wynne-Jones, S., Thomas, D. G. & Harding, S. E. (1992). Methods for off-line analysis of sedimentation velocity and sedimentation equilibrium patterns. In *Analytical Ultracentrifugation in Biochemistry and Polymer Science*, eds. S. E. Harding, A. J. Rowe & J. C. Horton. Chapter 5, Royal Society of Chemistry, Cambridge, UK.

Schachman, H. K. (1959). *Ultracentrifugation in Biochemistry.* Academic Press, New York.

Tanford, C. (1961). *Physical Chemistry of Macromolecules*, Chapter 6. John Wiley and Sons, New York.

Van Holde, K. E. (1985). *Physical Biochemistry* (2nd. Edn). Prentice Hall, New Jersey.

Yphantis, D.A. (1964). Equilibrium ultracentrifugation of dilute solutions. *Biochemistry,* **3,** 297–317.

Waaler, P.J., Arnesen, K., Graffner, C. & Müller, B.W. (1992). *Acta Pharm. Nord.*, **4,** 291.